

Article

Floatability of Fluorite and Calcite Inhibited by Sodium Hexametaphosphate via Ultrasonic Activation

Zhehui Yang ^{1,2,*}, Maolin Li ^{1,2,3}, Yingxin Lin ⁴, Wei Yao ^{1,2}, Yue Wu ^{1,2} and Rui Cui ^{1,2,*}

¹ College of Resources and Environmental Engineering, Wuhan University of Science and Technology, Wuhan 430081, China; 13974851980@vip.163.com (M.L.); yaowei1990520@163.com (W.Y.); 15225062811@163.com (Y.W.)

² Hubei Key Laboratory for Efficient Utilization and Agglomeration of Metallurgical Mineral Resources of Wuhan University of Science and Technology, Wuhan 430081, China

³ Changsha Research Institute of Mining and Metallurgy Limited Liability Company, Changsha 410012, China

⁴ School of Chemical & Environment Engineering, China University of Mining and Technology (Beijing), Beijing 100083, China; 18703848899@163.com

* Correspondence: yangzhehui_0722@163.com (Z.Y.); cuirui@wust.edu.cn (R.C.)

Abstract: In order to separate fluorite and calcite inhibited in tungsten tailings, the effect and mechanism of using ultrasonic external field activation to separate fluorite and calcite inhibited by sodium hexametaphosphate in a sodium oleate system were investigated. After pretreatment with an ultrasonic external field with a frequency of 40 kHz and sound intensity of 0.56, 0.50 and 0.40 W/cm², the flotation recovery of calcite could be increased from 16.08% to about 80%, while the flotation recovery of fluorite was only increased from 7.5% to about 20%, with a difference of 60% between the two flotation recoveries, and the larger the sound intensity, the shorter the pretreatment time and the smaller the ultrasonic input energy. The contact angle of the calcite surface increased, sodium oleate adsorption increased, and zeta potential decreased after ultrasonic pretreatment, while the contact angle, sodium oleate adsorption, and zeta potential of fluorite surface were less changed. The results of heat of adsorption and XPS measurements showed that more heat was released from the interaction between sodium hexametaphosphate and fluorite, and the Ca2p peaks on the surface of fluorite were shifted to a greater extent after the interaction, which inferred that the adsorption of fluorite and sodium hexametaphosphate was relatively easier and stronger. It is presumed that the ultrasonic pretreatment can bring the mineral surface to different degrees of desorption according to the adsorption strength of sodium hexametaphosphate, exposing Ca²⁺ active sites for sodium oleate adsorption, while expanding the floatability difference between fluorite and calcite.

Keywords: ultrasonic pretreatment; sodium hexametaphosphate; sodium oleate; fluorite; calcite



Citation: Yang, Z.; Li, M.; Lin, Y.; Yao, W.; Wu, Y.; Cui, R. Floatability of Fluorite and Calcite Inhibited by Sodium Hexametaphosphate via Ultrasonic Activation. *Minerals* **2023**, *13*, 1504. <https://doi.org/10.3390/min13121504>

Academic Editor: Przemyslaw B. Kowalczyk

Received: 23 October 2023

Revised: 23 November 2023

Accepted: 27 November 2023

Published: 30 November 2023



Copyright: © 2023 by the authors. Licensee MDPI, Basel, Switzerland. This article is an open access article distributed under the terms and conditions of the Creative Commons Attribution (CC BY) license (<https://creativecommons.org/licenses/by/4.0/>).

1. Introduction

Scheelite is often associated with calcium- and magnesium-bearing minerals such as fluorite and calcite [1]. In the flotation process of scheelite, phosphate agents are often added to inhibit the associated gangue mineral, and sodium oleate is used as a collector to preferentially achieve scheelite flotation [2–4]; while the flotation separation of the inhibited fluorite, calcite and other gangue minerals usually requires tailings re-treatment and the addition of other agents for selective activation [5], mostly by regrinding the tailings and adding acidized water glass [6] or adding sulfuric acid to activate fluorite and using new collectors [7], such as tailings pretreatment and continuous addition of chemical agents. As these methods are prone to environmental pollution, flotation backwater requires deep treatment before reuse and high energy consumption for regrinding pretreatment and other impacts, so that the pressure on safety and environmental management in actual production is high.

In recent years, physical external field regulation methods such as ultrasonics, microwaves, and magnetization have been widely used in the field of flotation [8–11]. Many researchers have carried out modulation via ultrasonic pretreatment of chemical agents, ultrasonic pretreatment of minerals, and ultrasonic pretreatment of slurry in order to enhance selective adsorption of chemical agents and improve mineral flotation recovery.

Huang Zheyu et al. [12] found that ultrasonic pretreatment of the collector could increase the conductivity of the collector solution, change the microstructure of the collector solution, increase the collector adsorption of minerals, and improve the flotation recovery of minerals. Gungoren et al. [13] studied the effect of ultrasonic waves on quartz in a dodecylamine hydrochloride flotation system, and flotation tests found that at 30 W ultrasonic waves, the quartz flotation recovery increased, but at 150 W ultrasound, the quartz flotation recovery decreased instead. Related tests showed that ultrasonic waves have a certain effect on the surface morphology of the particles and can increase the adsorption density of agents on the mineral surface and reduce the attachment time of bubbles to mineral particles. Shi Jia et al. [14] used an ultrasonic external field to act on the inhibited calcite in the water glass system, and the flotation recovery of calcite was increased from 8.50% to 82.73% after 15 min treatment of 40 kHz and a 150 W ultrasonic external field. Related tests showed that ultrasonic treatment could change the adsorption state of the agent on the mineral surface and modulate the floatability of the mineral. Guo Pingsheng et al. [15] found that ultrasound could accelerate the desorption of phenol on the desorption resin, and it was shown via calculation that the adsorbed phase molecules could obtain more energy through ultrasound, and their desorption rate was related to each material parameter of the adsorption system, ultrasonic field frequency, and ultrasonic field energy flow, and the higher the frequency and energy flow, the faster the resolution rate.

As described in the above literature, ultrasound can be applied as a form of external control in the field of mineral processing, and it is known that ultrasonic pretreatment can change the adsorption state of solid–liquid phase substances through desorption of adsorbed phase molecules, thus affecting mineral hydrophobicity, though this has not yet been applied in mineral separation, let alone in slurry systems where inhibitors and collectors coexist to achieve separation. In this paper, we investigated the effect of ultrasonic pretreatment on the flotation separation of two minerals via ultrasonic pretreatment of the inhibited fluorite and calcite in the sodium hexametaphosphate system and investigated the separation mechanism of ultrasonic pretreatment via contact angle, sodium oleate adsorption, zeta potential, heat of adsorption, and XPS. We further improved the explanation of ultrasound mechanism and provided certain technical support for the application of ultrasound as a green and efficient external field control method in practical production.

2. Test Samples and Research Methods

2.1. Test Samples and Experimental Agents

The fluorite and calcite used in the experiment were purchased from Ye's Ore Specimen Shop. The experimental ore samples were crushed manually, dry ground using a ceramic ball mill, and finally, $-74 + 38 \mu\text{m}$ particle size was obtained by vibrating a sieve machine for single mineral flotation. Figure 1 shows the XRD analysis results of fluorite and calcite, and Table 1 shows the chemical composition analysis results of fluorite and calcite, it can be seen from the graphs that the purchased fluorite and calcite have high purity and meet the requirements of a single mineral flotation test.

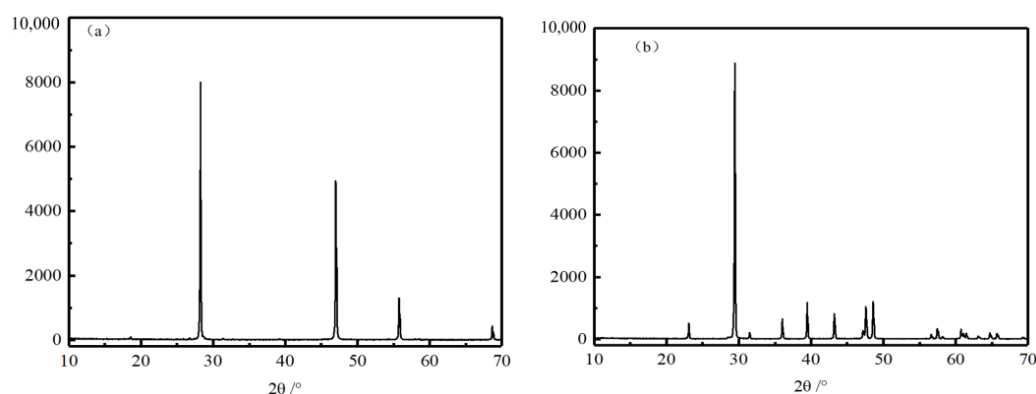


Figure 1. Fluorite and calcite XRD atlases. (a) Fluorite, (b) calcite.

Table 1. Analysis of single mineral chemical composition of fluorite and calcite (wt.%).

Sample Name	CaF ₂	CaO	SiO ₂	MgO	Al ₂ O ₃	Purity
Fluorite	99.14	-	0.39	0.13	0.18	99.14
Calcite	-	55.03	0.88	0.37	0.15	98.30

The test water was deionized water, and the agents used in the test are shown in Table 2.

Table 2. Experiment reagent.

Pharmacy Name	Molecular Formula	Grade	Manufacturers
Hydrochloric acid	HCl	Analysis pure	Sinopharm Group Chemical Reagent Co., Beijing, China
Sodium hydroxide	NaOH	Analysis pure	Sinopharm Group Chemical Reagent Co., Beijing, China
Sodium hexametaphosphate	(NaPO ₃) ₆	Chemically pure	Sinopharm Group Chemical Reagent Co., Beijing, China
Sodium oleate	C ₁₇ H ₃₃ COONa	Analysis pure	Shanghai Maikun Chemical Co., Shanghai, China
Potassium chloride	KCl	Analysis pure	Sinopharm Group Chemical Reagent Co., Beijing, China

2.2. Single Mineral Flotation Test

The flotation test was carried out on an XFGC hanging tank flotation machine with a spindle speed of 1680 r/min. First, 2.0 g of the test sample of $-74 + 38 \mu\text{m}$ particle size was weighed and placed in a 40 mL flotation tank, and 35 mL of deionized water was added to start agitation. As shown in the flotation flow chart in Figure 2, after adding reagents (the inhibitor was 1 g/L sodium hexametaphosphate, and the collector was 2 g/L sodium oleate) according to the steps, the flotation cell was moved to an ultrasonic cleaning machine (DSA150-GL1-3.8L) for ultrasonic pretreatment, and flotation was carried out after ultrasonic pretreatment. During the ultrasonic pre-treatment process, circulating cooling water was used in the ultrasonic generator to ensure that the temperature inside the flotation cell did not change, in order to eliminate the impact of ultrasonic temperature changes. The concentrate and tailings were filtered, dried, and weighed separately, and the recovery was calculated. The flotation recovery of single minerals was calculated according to Equation (1).

$$\varepsilon = \frac{m_1}{m_1 + m_2} \quad (1)$$

where, “ ε ” is the flotation recovery/%; “ m_1 ” and “ m_2 ” are the concentrate and tailings mass/g, respectively.

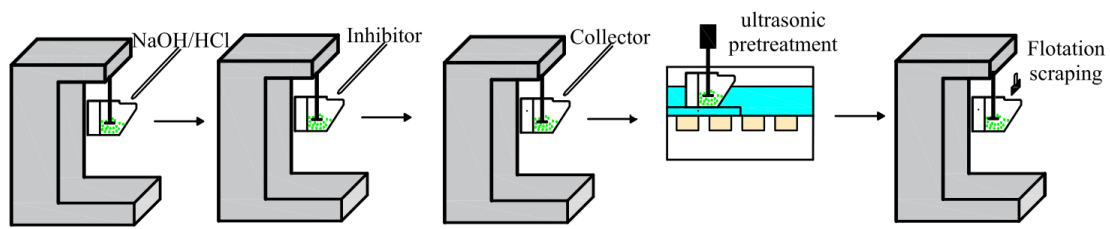


Figure 2. Flotation flow chart.

When the flotation cell was pretreated in the ultrasonic external field, the ultrasonic sound intensity was monitored in real time using an ultrasonic sound intensity meter, as shown in Figure 3, and adjusted to 0.56, 0.50, and 0.40 W/cm², respectively, to investigate the effect of different sound intensity of the ultrasonic external field input energy and time on the recovery of single-mineral flotation.

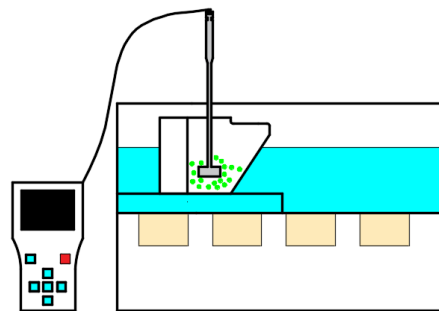


Figure 3. Ultrasonic sound intensity measurement.

2.3. Contact Angle Measurement

The sample was filtered and dried for testing after the basic mineral flotation test procedure with chemical agents addition and ultrasonic pretreatment; the dry powder samples were pressed and measured using the Dataphysics OCA20 contact angle meter. Each sample was repeated three times and the average value was used as the contact angle θ of the sample.

2.4. Determination of Sodium Oleate Adsorption on Mineral Surfaces

Different concentrations of sodium oleate solutions were prepared, and the absorbance was measured at 225 nm with the aid of an ultraviolet spectrophotometer (UV2550, Shimadzu, Kyoto, Japan), and the standard curve of sodium oleate was plotted. The solution in the single mineral flotation experimental tank was taken and put into a centrifuge for centrifugation at 2000 r/min for 15 min, the clear solution was taken for absorbance measurement, and the amount of sodium oleate adsorbed on the mineral surface was deduced from the sodium oleate concentration in the standard curve of sodium oleate (as shown in Figure 4) according to Equation (2).

$$\tau = 304.4 \frac{C_0 - C_1}{m} V \quad (2)$$

where, “ τ ” is the amount of sodium oleate adsorbed on the mineral surface/(mg/g); C_0 is the concentration of trap in the pulp before the reaction between mineral and reagents/(mg/L); C_1 is the concentration of trap in the pulp after the reaction between mineral and reagents/(mg/L); “ V ” is the volume of pulp/L; “ m ” is the mass of single mineral/g.

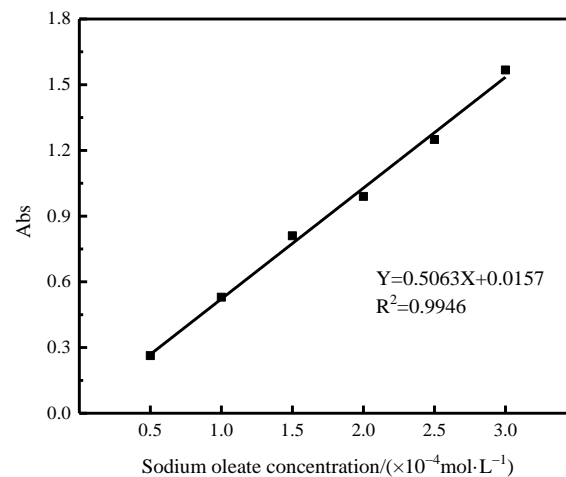


Figure 4. Sodium oleate concentration and absorbance label curve.

2.5. Zeta Potential Measurement

The minerals were finely ground to $-5 \mu\text{m}$ as the mineral zeta potential test sample, and 50 mg of sample was weighed for each determination. The instrument used for the test was the Zetasizer Nano ZS90 zeta potential meter from Malvern, U.K. Each sample was repeated three times and the average value was taken as the final result.

2.6. Heat of Adsorption Measurement

The fluorite and calcite samples were placed in NaOH solution with $\text{pH} = 9$, and 1 mL of the suspension was placed in the glass outer tube, 0.5 mL of sodium hexametaphosphate solution was added to the inner tube, and the inner and outer tubes were combined into the measurement cell. The same solution was added to the reference cell but not to the mineral sample. The RD496-2000 microcalorimeter was used for microcalorimetry. The temperature parameter 298.15 K was set, and when the baseline was smooth, the inner glass tube was poked and the trace heat change was measured, and each group of tests was repeated three times and the average value was taken. And the kinetic constants were calculated by the analysis of Equation (3).

$$\ln\left(\frac{1}{H_{\infty}} \frac{dH_i}{dt}\right) = \ln k + n \ln\left(1 - \frac{H_i}{H_{\infty}}\right) \quad (3)$$

where H_{∞} is the total heat/mJ, H_i is the heat/mJ at time t , k is the reaction rate constant/ s^{-1} , and n is the number of reaction stages.

2.7. XPS Measurement

The minerals were filtered and rinsed three times with deionized water, and finally dried in an oven at low temperature ($60 \text{ }^{\circ}\text{C}$), and finally detected by XPS using the Thermo Scientific K-Alpha model X-ray photoelectron spectrometer. The original, suppressed and ultrasonically pretreated samples of the two minerals were measured separately.

3. Experimental Results and Mechanistic Analysis

3.1. Determination of Pharmacological Regime

The experimental agent probe test is shown in Figure 5 for pH test, sodium oleate dosage test, and sodium hexametaphosphate dosage test.

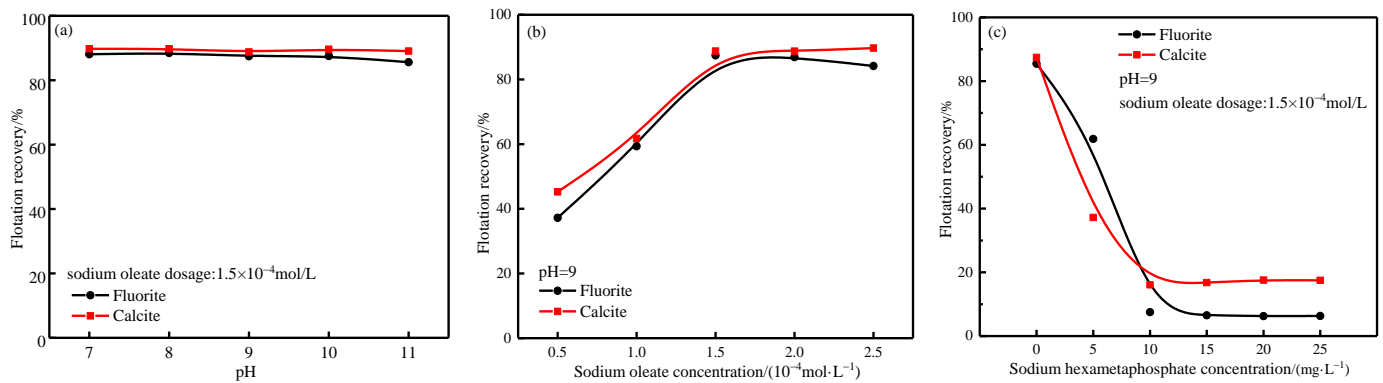


Figure 5. Flotation agent system. (a) pH test, (b) sodium oleate dosage test, (c) sodium hexametaphosphate dosage test.

In order to simulate the chemical environment required for preferential flotation of scheelite with tungsten tin polymetallic-associated fluorite ore, it is necessary to first suppress both fluorite and calcite. From Figure 5b, it can be seen that in the sodium oleate (NaOL) dosage of 1.5×10^{-4} mol/L, both fluorite and calcite have good floatability. It was finally determined that the fluorite flotation recovery was only 7.5% and calcite flotation recovery was 16.08% under the pharmaceutical system of pH = 9, sodium hexametaphosphate (SHMP) dosage of 10 mg/L and sodium oleate (NaOL) dosage of 1.5×10^{-4} mol/L. Both minerals are significantly inhibited, and the chemical environment of the solution is also suitable for enrichment of scheelite [7].

3.2. Single Mineral Ultrasonic Pretreatment Test

The effect of pretreatment time and input energy of ultrasonic external field with different sound intensity on the recovery of single mineral flotation is shown in Figures 6 and 7.

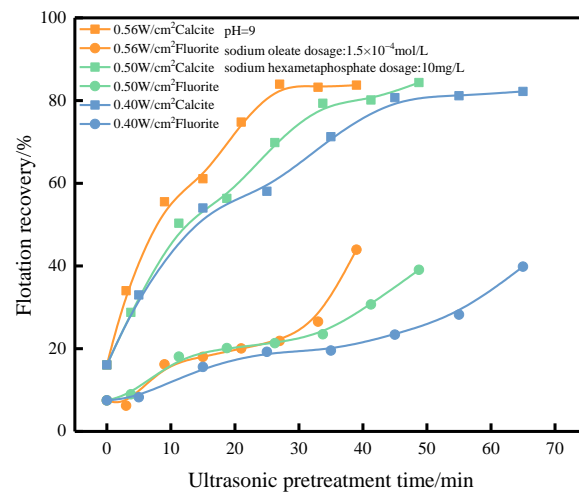


Figure 6. Effect of ultrasonic pretreatment time on flotation recovery.

As shown in Figure 6, the flotation recoveries of fluorite and calcite were found to rise first and then stabilize with the increase in the pretreatment time. The flotation recovery of fluorite increased slowly with the increase in the ultrasonic pretreatment time, and the flotation recovery of fluorite reached 21.87%, 23.49%, and 23.40% after pretreatment at 0.56, 0.50, and 0.40 W/cm² for 27, 33.75, and 45 min. The difference between the flotation recoveries of fluorite and calcite could reach about 60% after pretreatment in the ultrasonic field of one of the sound intensities for a certain time.

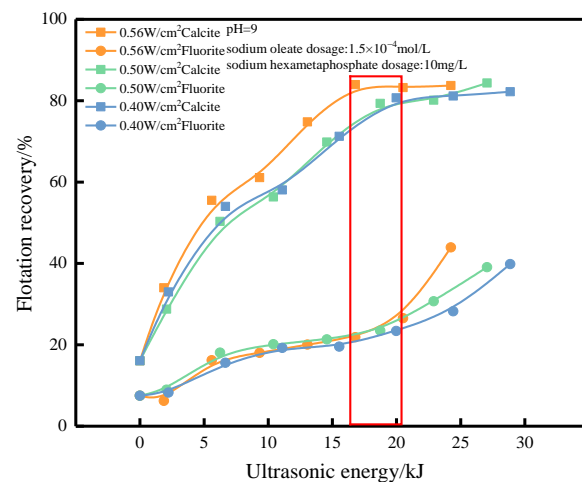


Figure 7. Effect of ultrasonic energy on flotation recovery.

The differences in flotation recoveries of fluorite and calcite were greatest at 27, 33.75 and 45 min of pretreatment, with 0.56, 0.50 and 0.40 W/cm² of ultrasonic external field used in the experiment. At this time, the input energy of ultrasonic field was calculated based on the sound intensity, pretreatment time, and flotation tank bottom area, and the input energy of the ultrasonic field was 16.78, 18.73 and 19.98 kJ (The specific points corresponding to the flotation recovery rate of energy have been boxed in the figure). However, the flotation recovery of calcite did not change significantly when more energy was input to the ultrasonic field, while fluorite could still be activated, or with the increase in pretreatment time and input energy. The fluorite gradually activated, the floatability improved, and the flotation recovery increased.

In the experimental ultrasonic field, it was found that the minerals could be activated in the ultrasonic field with different sound strengths and the activation trend was more or less the same, but the activation speed was different, and the pretreatment time required to improve the floatability of minerals shortened as the sound strength of the ultrasonic field increased. At the same time, in the case that the minerals are pretreated by ultrasonic external field with different sound intensity and the activation achieves the same flotation recovery, the larger the ultrasonic external field sound intensity, the smaller the energy input to the flotation tank from the ultrasonic external field. In other words, the greater the ultrasonic field intensity, the shorter the mineral pretreatment time and the lower the input energy, which can achieve the effect of efficient activation and cost saving. Perhaps this is because high sound intensity ultrasonic fields can release an enormous amount of energy in a short period of time, causing the surface agents of minerals to desorb, while low sound intensity may do more useless work.

3.3. Contact Angle Measurement

Taking the ultrasonic external field of 40 kHz and 0.56 W/cm² as an example, the contact angle angles of fluorite and calcite at different treatment stages are shown in Figure 8.

As can be seen from Figure 8, compared to the original ore, the contact angle of fluorite and calcite slightly decreased after the sequential addition of sodium hexametaphosphate and sodium oleate. After 27 min of ultrasonic external pretreatment, the contact angle of calcite increased significantly from 23.7° to 89.6°, while the contact angle of fluorite only increased from the inhibited 11.4° to 28.7°. It is known that the hydrophobicity of calcite surface can be greatly improved by ultrasonic pretreatment, which improves the floatability of calcite and enlarges the flotation difference between fluorite and calcite. The specific contact angle images are shown in Figure 8.

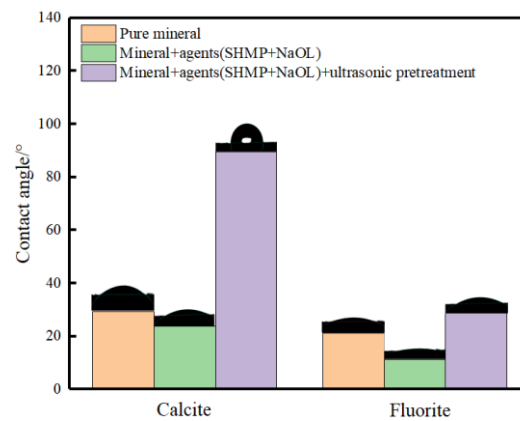


Figure 8. Contact angles for each treatment stage of the mineral.

3.4. Sodium Oleate Adsorption

Taking the ultrasonic external field of 40 kHz and 0.56 W/cm² as an example, the flotation test agent regime was: pH = 9, sodium hexametaphosphate dosage of 10 mg/L and sodium oleate dosage of 1.5×10^{-4} mol/L. The ultrasonic pretreatment time on the adsorption of sodium oleate on the surface of fluorite and calcite is shown in Figure 9.

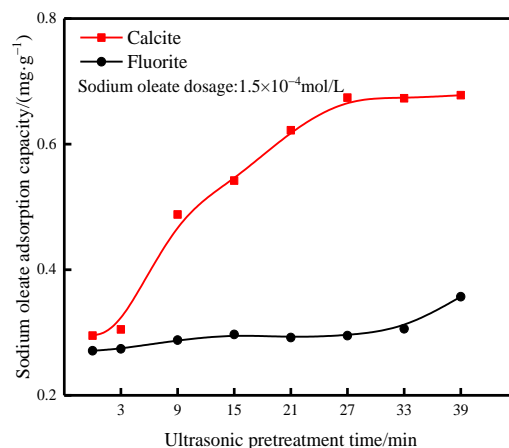


Figure 9. Adsorption of sodium oleate on the surface of fluorite and calcite.

As can be seen from Figure 9, the adsorption amount of sodium oleate on calcite surface increased significantly with the increase in ultrasonic pretreatment time; the adsorption amount of sodium oleate on calcite surface increased from 0.29 mg/g without ultrasonic pretreatment to 0.67 mg/g when the ultrasonic pretreatment time reached 27 min, while the adsorption amount of sodium oleate on fluorite surface only increased from 0.27 mg/g without ultrasonic pretreatment to 0.29 mg/g at 27 min, which did not improve significantly.

Therefore, ultrasonic pretreatment can change the adsorption state of the agent on the mineral surface, thus affecting the adsorption amount and contact angle change of the agent.

3.5. Zeta Potential Measurement

The ultrasonic external field of 40 kHz and 0.56 W/cm² was used to determine the surface zeta potential of two minerals in the single-agent pulp, the inhibited pulp and the ultrasonic pretreatment-inhibited pulp using the zeta potential meter, and the results are shown in Figure 10.

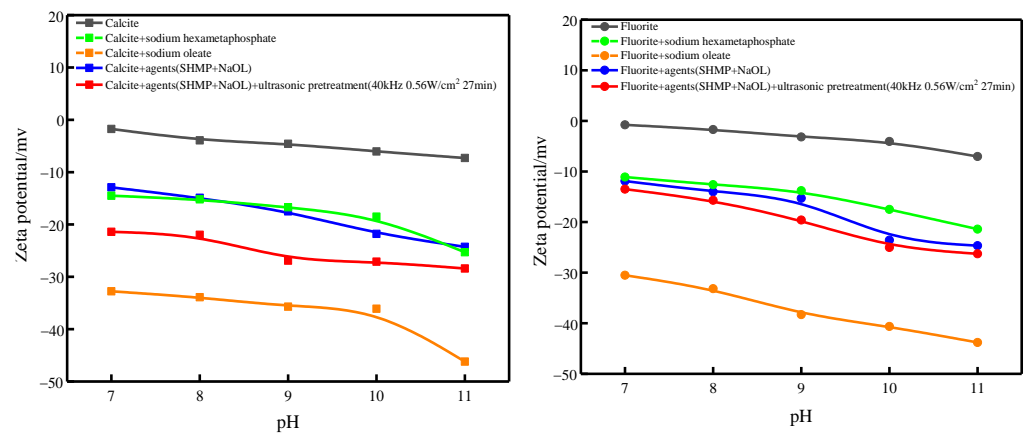


Figure 10. Zeta potential of mineral surface.

As can be seen from Figure 10, the fluorite and calcite zeta potentials shifted toward negative potentials when sodium hexametaphosphate and sodium oleate were added alone.

After ultrasonic pretreatment of the inhibited calcite, the calcite surface zeta potential shifted toward the surface zeta potential of sodium oleate alone compared to that of the inhibited calcite without ultrasonic pretreatment, which presumably led to the change in calcite surface zeta potential via desorption of sodium hexametaphosphate on the calcite surface and exposure of new active sites for sodium oleate adsorption.

The zeta potential of fluorite with sodium hexametaphosphate alone and without ultrasonic pretreatment are similar. After ultrasonic pretreatment of the inhibited fluorite, the surface zeta potential of fluorite did not change much, and it is presumed that the adsorption state of the agent on the surface of fluorite did not change.

3.6. Heat of Adsorption Measurement

The heat of adsorption curves of fluorite, calcite, and sodium hexametaphosphate and their kinetic parameters were tested using a microcalorimeter, as shown in Table 3 and Figure 11.

Table 3. Adsorption thermokinetic parameters.

Mineral Sample Name	Q/mJ	k/×10 ⁻² s ⁻¹	n	R ²	(dH/dt) _{max} /(mJ·s ⁻¹)
Calcite	102	6.99	0.6824	0.9920	0.1639
Fluorite	191.1	7.73	0.9110	0.9932	0.3726

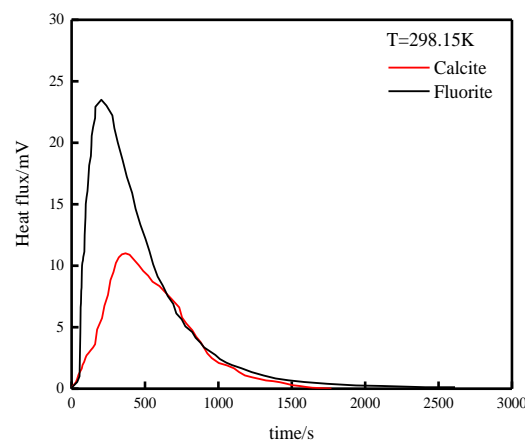


Figure 11. Adsorption heat curve.

From Figure 11, it can be seen that the reactions of fluorite, calcite, and sodium hexametaphosphate are all exothermic reactions. The relevant adsorption thermodynamic data can be obtained by analyzing and calculating the heat of adsorption curve of Figure 11 through Equation (3). As shown in Table 3, fluorite reacts with sodium hexametaphosphate with $Q = 191.1 \text{ mJ}$, while calcite reacts with sodium hexametaphosphate with $Q = 102 \text{ mJ}$, so fluorite is easier to react with sodium hexametaphosphate, and sodium hexametaphosphate adsorbs more firmly on the surface of fluorite than calcite. Meanwhile, the reaction rate constant $k = 7.73 \times 10^{-2} \text{ s}^{-1}$ of fluorite and sodium hexametaphosphate is larger than that of calcite and sodium hexametaphosphate $k = 6.99 \times 10^{-2} \text{ s}^{-1}$, so the adsorption rate of fluorite and sodium hexametaphosphate is faster.

3.7. XPS Measurement

Taking the ultrasonic external field at 40 kHz and 0.56 W/cm^2 as an example, the full XPS spectra of the two mineral surfaces and their elemental contents are shown in Figure 12, and the Ca2p fine spectral fractions and their binding energies are shown in Figure 13 and Table 4.

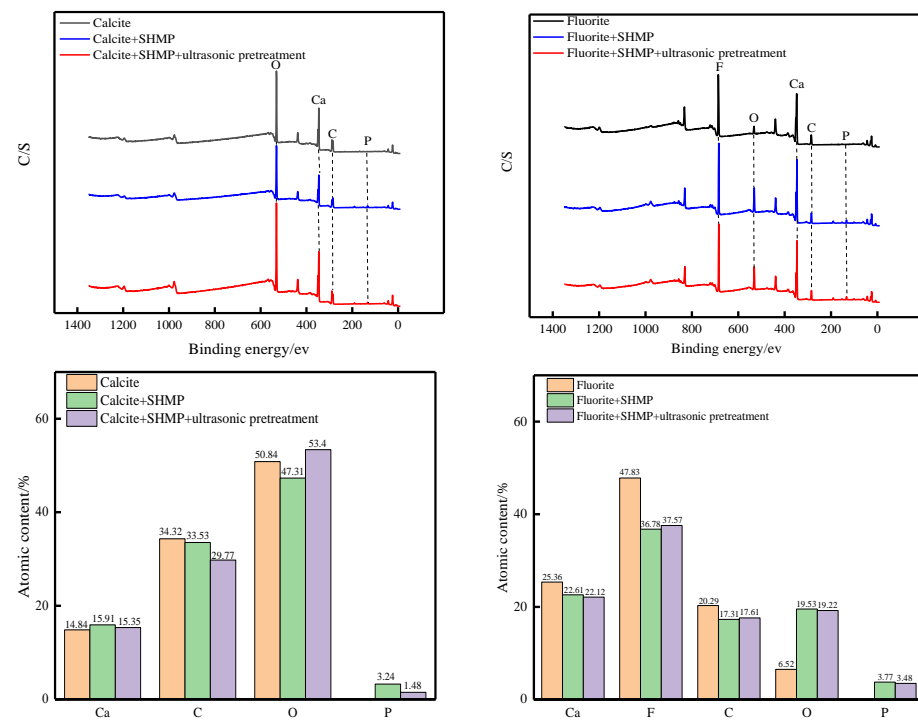


Figure 12. XPS full spectrum and element content of minerals.

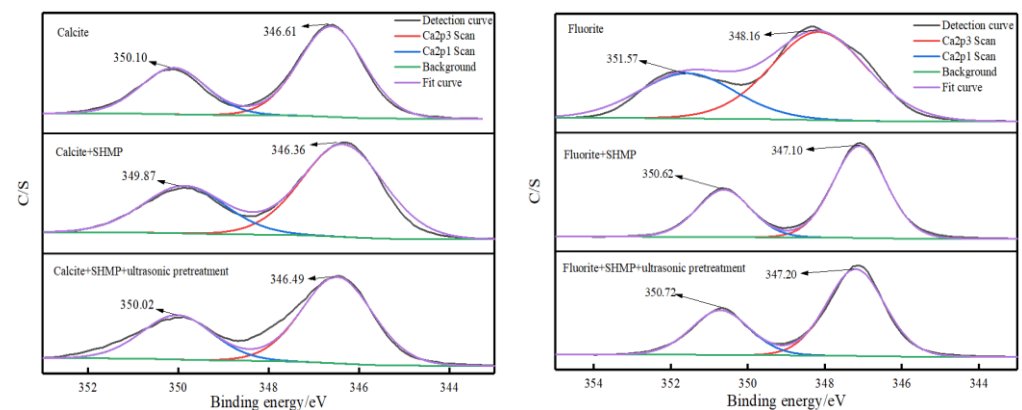


Figure 13. Fine spectral peak fitting diagram of mineral Ca2p.

Table 4. Characteristic peak of mineral Ca2p.

Samples	Ca2p	Raw Ore/eV	+SHMP	ΔeV (Compared to Raw Ore)	+SHMP +Ultrasonic Pretreatment	ΔeV (Compared to Raw Ore)
Calcite	Ca2p1/2	350.10	349.87	0.23	350.02	0.08
	Ca2p3/2	346.61	346.36	0.25	346.69	0.08
Fluorite	Ca2p1/2	351.57	350.62	0.95	350.72	0.85
	Ca2p3/2	348.16	347.10	1.06	347.20	0.96

Sodium hexametaphosphate chelates with calcium ions on the mineral surface and adsorbs on the calcite and fluorite surfaces [16]. From the full XPS spectrum in Figure 12, it is clear that the P2p characteristic peaks appear on the surfaces of fluorite and calcite after the interaction of minerals with sodium hexametaphosphate, indicating that sodium hexametaphosphate is adsorbed on the surfaces of both minerals. However, it can be seen from the distribution of elemental content in Figure 12 that calcite surface P elemental content decreased from 3.24% to 1.48% after ultrasonic pretreatment, while fluorite surface P elemental content changed very little after ultrasonic pretreatment, so sodium hexametaphosphate on calcite surface was desorbed at 27 min of ultrasonic pretreatment, while sodium hexametaphosphate on the fluorite surface was not desorbed.

From Figure 13 and Table 4, it can be seen that after the addition of sodium hexametaphosphate to the original ore, the deviation of the Ca2p characteristic peak of fluorite compared with the original ore is much larger than that of calcite, which means that the action of sodium hexametaphosphate with fluorite is stronger than that of calcite, and the deviation of the Ca2p characteristic peak of calcite compared with the original ore after ultrasonic pretreatment is within the measurement error of the instrument, while the deviation of fluorite is still larger.

Therefore, XPS can prove that the mechanism of ultrasonic pretreatment is that ultrasonic waves can desorb sodium hexametaphosphate on the surface of minerals, so that new active sites are exposed. As fluorite interacts with sodium hexametaphosphate more strongly than calcite, sodium hexametaphosphate on calcite surface is preferentially desorbed, while sodium hexametaphosphate on fluorite surface needs more energy to be desorbed.

3.8. Mechanistic Model Prediction

The predicted ultrasonic pretreatment mechanism model is shown in Figure 14.

First, after adding sodium hexametaphosphate and sodium oleate successively, Ca^{2+} on the surfaces of fluorite and calcite reacted with sodium hexametaphosphate first, resulting in insufficient Ca^{2+} active sites on the mineral surfaces for sodium oleate adsorption, and fluorite and calcite were inhibited. After adding the ultrasonic field for ultrasonic pretreatment, ultrasonic pretreatment mainly releases a large amount of energy through the collapse of cavitation bubbles formed by ultrasonic cavitation, causing the bond formed between minerals and sodium hexametaphosphate to break, thereby causing sodium hexametaphosphate to desorb from the mineral surface, and the adsorption strength of sodium hexametaphosphate on the surfaces of fluorite and calcite minerals was different, resulting in different degrees of sodium hexametaphosphate desorption on the surfaces of the two minerals. The fluorite surface had less sodium hexametaphosphate desorption and no sodium oleate adsorption sites. Finally, the selective separation of the two minerals was achieved via the ultrasonic external pretreatment.

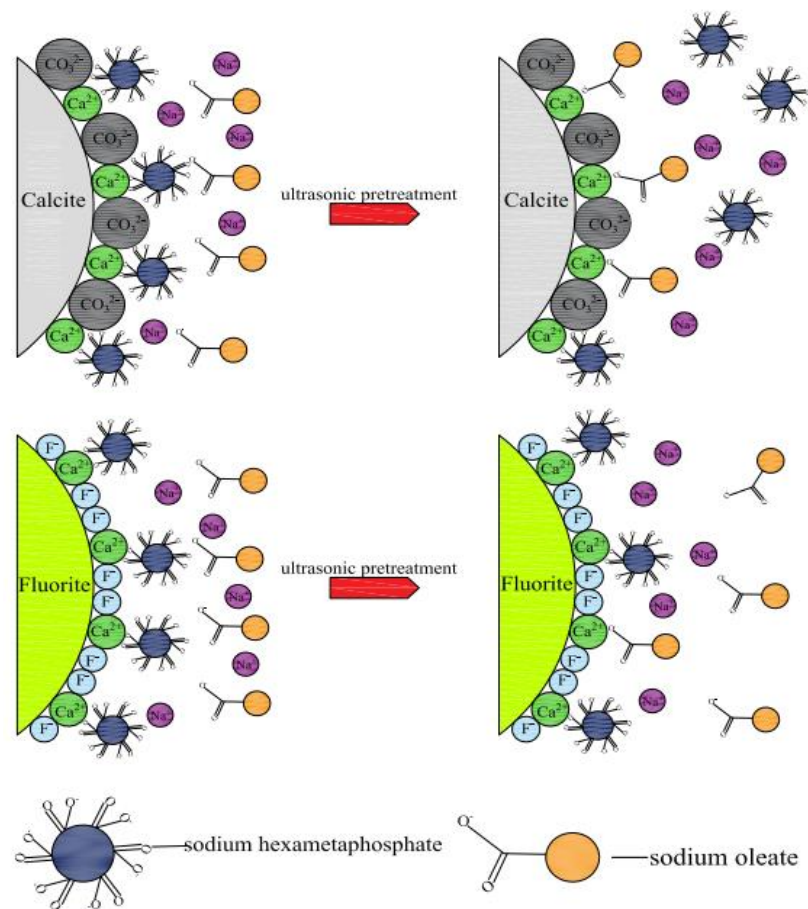


Figure 14. Mechanism model of ultrasonic pretreatment.

4. Conclusions

This article found that ultrasonic pre-treatment achieves an activation effect by breaking the bonds generated between reagents and minerals. However, the strength of the bonds generated between the two is described by macroscopic adsorption heat and qualitative peak shift. It is necessary to quantify the strength of the bonds generated between reagents and minerals through more accurate detection methods. Further research is needed on the quantitative relationship between bond strength and cavitation. However, this article adds a reserve technique for the flotation of fluorite in tungsten tin polymetallic-associated fluorite mines.

1. Ultrasonic pretreatment of fluorite and calcite inhibited in the sodium hexametaphosphate system, with pH = 9, 10 mg/L sodium hexametaphosphate and 1.5×10^{-4} mol/L sodium oleate, the calcite flotation recovery was only 16.08% without ultrasonic pretreatment. The calcite flotation recovery increased to about 80% due to pretreatment with ultrasonic external fields at 40 kHz, 0.56, 0.50 and 0.40 W/cm² for 27, 33.75 and 45 min, respectively, while the fluorite flotation recovery only increased from 7.5% to 20% without ultrasonic pretreatment. The difference between the two flotation recoveries was 60%.
2. Minerals can be activated in the ultrasonic field with different sound strengths and their activation trends are more or less the same, but the activation rate is different. The greater the increase in the sound strength of the ultrasonic field, the shorter the pretreatment time required to improve the floatability of minerals. At the same time, if the minerals are pretreated using an ultrasonic external field with different sound intensity and the activation achieves the same flotation recovery, the larger the ultrasonic external field sound intensity, the smaller the energy input to the flotation

tank from the ultrasonic external field. In other words, the greater the ultrasonic field intensity, the shorter the mineral pretreatment time and the lower the input energy, which can achieve the effect of efficient activation and cost saving.

3. Through contact angle measurement, sodium oleate adsorption, zeta potential, heat of adsorption measurement, and XPS measurement, it can be found that because sodium hexametaphosphate and fluorite act more strongly than calcite, pretreatment via regulating the ultrasonic external field can preferentially desorb sodium hexametaphosphate on the surface of calcite, while sodium hexametaphosphate on the surface of fluorite takes longer time to desorb. The adsorption of sodium hexametaphosphate on calcite surface exposed new active sites for sodium oleate adsorption, which increased the adsorption amount of sodium oleate from 0.29 mg/g to 0.67 mg/g, decreased the surface zeta potential, and increased the contact angle, while the contact angle, sodium oleate adsorption amount, and zeta potential on the fluorite surface did not change significantly.

Author Contributions: Conceptualization, R.C. and Z.Y.; validation, Z.Y., Y.L. and Y.W.; writing—review and editing, M.L., W.Y. and R.C. All authors have read and agreed to the published version of the manuscript.

Funding: This research was funded by the Knowledge Innovation Project of Wuhan Science and Technology Bureau (2023020201020411), “the 14th Five Year Plan” Hubei Provincial advantaged characteristic disciplines (groups) project of Wuhan University of Science and Technology (2023A0401).

Data Availability Statement: Data are contained within the article. The data are not publicly available due to the project needs further progress, so it is temporarily kept confidential.

Acknowledgments: The authors would like to thank Shiyanjia Lab (www.shiyanjia.com) for providing the XPS tests.

Conflicts of Interest: Maolin Li was employed by the company Changsha Research Institute of Mining and Metallurgy Limited Liability Company. The remaining authors declare that the research was conducted in the absence of any commercial or financial relationships that could be construed as a potential conflict of interest.

References

1. Ghosh, U.; Upadhyay, D. The retrograde evolution of F-rich skarns: Clues from major and trace element chemistry of garnet, scheelite, and vesuvianite from the Belka Pahar wollastonite deposit, India. *Lithos Int. J. Mineral. Petrol. Geochem.* **2022**, *422–423*, 106750. [[CrossRef](#)]
2. Foucaud, Y.; Collet, A.; Filippova, I.; Badawi, M.; Filippov, L. Synergistic effects between fatty acids and non-ionic reagents for the selective flotation of scheelite from a complex tungsten skarn ore. *Miner. Eng.* **2022**, *182*, 107566. [[CrossRef](#)]
3. Foucaud, Y.; Filippova, I.V.; Filippov, L.O. Investigation of the depressants involved in the selective flotation of scheelite from apatite, fluorite, and calcium silicates: Focus on the sodium silicate/sodium carbonate system. *Powder Technol. Int. J. Sci. Technol. Wet Dry Part. Syst.* **2019**, *352*, 501–512. [[CrossRef](#)]
4. Faramarzpour, A.; Samadzadeh Yazdi, M.R.; Mohammadi, B.; Chehreh Chelgani, S. Calcite Froth Flotation—A review. *J. Mater. Res. Technol.* **2022**, *19*, 1231–1241. [[CrossRef](#)]
5. Das, S.K.; Nagesh, C.H.R.V.S.; Sreenivas, T.; Kundu, T.; Angadi, S.I. A treatise on occurrence, beneficiation and plant practices of tungsten-bearing ores. *Powder Technol.* **2023**, *429*, 118938. [[CrossRef](#)]
6. Pereira, L.; Kupka, N.; Hoang, D.H.; Michaux, B.; Saquran, S.; Ebert, D.; Rudolph, M. On the impact of grinding conditions in the flotation of semi-soluble salt-type mineral-containing ores driven by surface or particle geometry effects? *Int. J. Min. Sci. Technol.* **2023**, *33*, 855–872. [[CrossRef](#)]
7. Jong, K.; Paek, I.; Kim, Y.; Li, I.; Jang, D. Flotation mechanism of a novel synthesized collector from *Evodiaefructus* onto fluorite surfaces. *J. Miner. Eng.* **2020**, *146*, 106017. [[CrossRef](#)]
8. Li, G.; Shi, J.; Fang, S.; Zhu, D.; Nie, D.; Cui, R. Study on the effect of ultrasonic wave on the floatability of calcite under water glass and sodium oleate system. *Conserv. Util. Miner. Resour.* **2021**, *41*, 131–138.
9. Mitra, S.; Hoque, M.M.; Evans, G.; Nguyen, A. Direct visualisation of bubble-particle interactions in presence of cavitation bubbles in an ultrasonic flotation cell. *Miner. Eng.* **2021**, *174*, 107258. [[CrossRef](#)]
10. Amankwah, R.; Ofori-Sarpong, G. Microwave roasting of flash flotation concentrate containing pyrite, arsenopyrite and carbonaceous matter. *Miner. Eng.* **2020**, *151*, 106312. [[CrossRef](#)]
11. Sobhy, A.; Lu, J.; Chen, L.; Ahmed, N. Development of magnetic flotation hybrid separation process for cleaner coal preparation. *Miner. Eng.* **2023**, *203*, 108372. [[CrossRef](#)]

12. Huang, Z. *Effect of Ultrasonic Wave on the Properties of Collector Solution and Its Adsorption with Scheelite, Fluorite and Calcite*; Jiangxi University of Science and Technology: Ganzhou, China, 2019.
13. Gungoren, C.; Ozdemir, O.; Wang, X.; Ozkan, S.; Miller, J. Effect of ultrasound on bubble-particle interaction in quartz-amine flotation system. *Ultrason. Sonochem* **2019**, *52*, 446–454. [[CrossRef](#)] [[PubMed](#)]
14. Shi, J.; Cui, R.; Ning, J.; Yao, W.; Sun, H.; Li, R.; Yang, Z. Study on the effect of ultrasonic cavitation on the flotation behavior of calcite. *Metal Mine*. **2022**, *548*, 120–125.
15. Guo, P.; Han, G.; Zhang, N.; Hua, B.; Li, Z. Mechanism and field synergy analysis of desorption rate by ultrasonic field intensification. *J. Chem. Eng. High. Educ.* **2006**, *2*, 300–305.
16. Kang, J.; Hu, Y.; Sun, W.; Gao, Z.; Liu, R. Utilization of Sodium Hexametaphosphate for Separating Scheelite from Calcite and Fluorite Using an Anionic–Nonionic Collector. *Minerals* **2019**, *9*, 705. [[CrossRef](#)]

Disclaimer/Publisher’s Note: The statements, opinions and data contained in all publications are solely those of the individual author(s) and contributor(s) and not of MDPI and/or the editor(s). MDPI and/or the editor(s) disclaim responsibility for any injury to people or property resulting from any ideas, methods, instructions or products referred to in the content.